Inorganic Chemistry
Article

*Inorg. Chem.* **2011**, *50*, 819–826 **819**
DOI: 10.1021/ic101227u

# Bonding Analysis of Metal−Metal Multiple Bonds in $R_3M-M'R_3$ (M, M′ = Cr, Mo, W; R = Cl, $NMe_2$)

**Nozomi Takagi,*,† Andreas Krapp,*,‡ and Gernot Frenking*,†**

†*Fachbereich Chemie, Philipps−Universität Marburg, Hans-Meerwein-Strasse, D-35039 Marburg, Germany, and* ‡*Center for Theoretical and Computational Chemistry, Department of Chemistry, University of Oslo, POB 1033, Blindern, N-0315 Oslo, Norway*

Received June 19, 2010

The bonding situation of homonuclear and heteronuclear metal−metal multiple bonds in $R_3M-M'R_3$ (M, M′ = Cr, Mo, W; R = Cl, $NMe_2$) is investigated by density functional theory (DFT) calculations, with the help of energy decomposition analysis (EDA). The M−M′ bond strength increases as M and M′ become heavier. The strongest bond is predicted for the 5*d*−5*d* tungsten complexes $(NMe_2)_3W-W(NMe_2)_3$ ($D_e$ = 103.6 kcal/mol) and $Cl_3W-WCl_3$ ($D_e$ = 99.8 kcal/mol). Although the heteronuclear molecules with polar M−M′ bonds are not known experimentally, the predicted bond dissociation energies of up to 94.1 kcal/mol for $(NMe_2)_3Mo-W(NMe_2)_3$ indicate that they are stable enough to be isolated in the condensed phase. The results of the EDA show that the stronger $R_3M-M'R_3$ bonds for heavier metal atoms can be ascribed to the larger electrostatic interaction caused by effective attraction between the expanding valence orbitals in one metal atom and the more positively charged nucleus in the other metal atom. The orbital interaction reveal that the covalency of the homonuclear and heteronuclear $R_3M-M'R_3$ bonds is due to genuine triple bonds with one $\sigma$- and one degenerate $\pi$-symmetric component. The metal−metal bonds may be classified as triple bonds where $\pi$-bonding is much stronger than $\sigma$-bonding; however, the largest attraction comes from the quasiclassical contribution to the metal−metal bonding. The heterodimetallic species show only moderate polarity and their properties and stabilities are intermediate between the corresponding homodimetallic species, a fact which should allow for the experimental isolation of heterodinuclear species. CASPT2 calculations of $Cl_3M-MCl_3$ (M = Cr, Mo, W) support the assignment of the molecules as triply bonded systems.

## Introduction

The chemistry of metal−metal multiple bonds has been extensively developed in the last few decades, after the first isolation of the anionic $[Re_2Cl_8]^{2-}$ in the $K_2[Re_2Cl_8]\cdot 2H_2O$ complex. It has a formal quadruple bond between the Re atoms with an $\sigma^2\pi^4\delta^2$ electron configuration.[1,2] Since then, many compounds that possess metal−metal multiple bonds have been synthesized and isolated, as summarized in the prominent book by Cotton, Murillo, and Walton.[3] In recent years, the chemistry of metal−metal multiple bonds has come into focus again, mainly because of the reports about very short metal−metal bonds with high bond orders,[4] triggered by Power's recent report about the very short Cr−Cr bond with a formal quintuple bond.[5] The latter bonding type was recently investigated with quantum chemical methods by Gagliardi and co-workers.[6] Early theoretical studies of compounds with metal−metal multiple bonds have been reported by groups led by Hall,[7] Davidson,[8] and others.[9] The latter studies focused on homodimetallic compounds.

In contrast to the numerous reports about homodinuclear metal−metal bonds, the chemistry of their heterodinuclear

*E-mails: takagi@chemie.uni-marburg.de (N.T.), andreas.krapp@kjemi.uio.no (A.K.), and frenking@chemie.uni-marburg.de (G.F.).

(1) Cotton, F. A.; Harris, C. B. *Inorg. Chem.* **1965**, *4*, 30.
(2) Cotton, F. A. *Inorg. Chem.* **1965**, *4*, 334.
(3) Cotton, F. A., Murillo, C. A., Walton, R. A., Eds. *Multiple Bonds Between Metal Atoms*, 3rd Edition; Springer Science and Business Media, Inc.: New York, 2005.
(4) (a) Kreisel, K. A.; Yap, G. P. A.; Dmitrenko, O.; Landis, C. R.; Theopold, K. H. *J. Am. Chem. Soc.* **2007**, *129*, 14162. (b) Noor, A.; Wagner, F. R.; Kempe, R. *Angew. Chem., Int. Ed.* **2008**, *47*, 7246. (c) Tsai, Y. C.; Hsu, C. W.; Yu, J. S. K.; Lee, G. H.; Wang, Y.; Kuo, T. S. *Angew. Chem., Int. Ed.* **2008**, *47*, 7250. (d) Hsu, C. W.; Yu, J. S. K.; Yen, C. H.; Lee, G. H.; Wang, Y.; Tsai, Y. C. *Angew. Chem., Int. Ed.* **2008**, *47*, 9933. (e) Horvath, S.; Gorelsky, S. I.; Gambarotta, S.; Korobkov, I. *Angew. Chem., Int. Ed.* **2008**, *47*, 9937.
(5) Nguyen, T.; Sutton, A. D.; Brynda, M.; Fettinger, J. C.; Long, G..J.; Power, P. P. *Science* **2005**, *310*, 844.
(6) (a) La Macchia, G.; Li Manni, G.; Todorova, T. K.; Brynda, M.; Aquilante, F.; Roos, B. O.; Gagliardi, L. *Inorg. Chem.* **2010**, *49*, 5216. (b) Brynda, M.; Gagliardi, L.; Roos, B. O. *Chem. Phys. Lett.* **2009**, *471*, 1.
(7) (a) Hall, M. B. *J. Am. Chem. Soc.* **1980**, *102*, 2104. (b) Kok, R. A.; Hall, M. B. *Inorg. Chem.* **1983**, *22*, 728.
(8) (a) Chisholm, M. N.; Davidson, E. R.; Huffmann, J. C.; Quinlan, K. B. *J. Am. Chem. Soc.* **2001**, *123*, 9652. (b) Chisholm, M. N.; Davidson, E. R.; Quinlan, K. B. *J. Am. Chem. Soc.* **2002**, *124*, 15351.
(9) (a) Connor, J. A.; Pilcher, G.; Skinner, H. A.; Chisholm, M. H.; Cotton, F. A. *J. Am. Chem. Soc.* **1978**, *100*, 7738. (b) Ziegler, T.; Tschinke, V.; Becke, A. *Polyhedron* **1987**, *6*, 685.


Published on Web 01/06/2011

**Table 1.** Nomenclature of the Compounds $R_3M-M'R_3$ (M, M′ = Cr, Mo, W; R = Cl, $NMe_2$)

| M | M′ | compound |
|---|---|---|
| Cr | Cr | **1R** |
| Mo | Mo | **2R** |
| W | W | **3R** |
| Cr | Mo | **4R** |
| Cr | W | **5R** |
| Mo | W | **6R** |

counterparts, which may have polar metal−metal bonds, is less developed, especially when it comes to multiply bonded systems. Heterodinuclear molecules with metal−metal single bonds are relatively well-studied experimentally; they are mainly compounds of the so-called "early-late" type.[10−13] These are of interest because of their potential as catalysts in metal-mediated reactions. However, there is only one well-developed class of compounds with heterodinuclear metal−metal multiple bonds that was described by Collmann and co-workers in their work on substituted metal porphyrin dimers in which two transition metals are multiply bonded to each other, as summarized in ref 14. The use of the porphyrin rings in the Collmann systems enforces the same local 4-fold symmetry of the metal−metal bond as in the prototypical $[Re_2Cl_8]^{2-}$. The bonding situation in the Collmann systems can thus be analyzed in comparison to that in $[Re_2Cl_8]^{2-}$ and the formal metal−metal bond order in the Collmanns systems ranges from quadruple bonds with an electron configuration of $\sigma^2\pi^4\delta^2$ as in $[Re_2Cl_8]^{2-}$ to electron-rich triple bonds with a formal configuration of, e.g., $\sigma^2\pi^4\delta^2\delta^{*2}$. These systems are very interesting; however, these will be the focus of an upcoming work.

Our interest in this work, however, will be on homonuclear and heterodinuclear metal−metal multiple bonded systems with electron-poor triple bonds with a formal $\sigma^2\pi^4$ electron configuration. Such a bonding situation is realized in molecules of the general formula $R_3M-M'R_3$, where the transition metals M and M′ have a formal electron count of $(d-d)^6$. Such systems are experimentally known, with M = M′ = Cr or Mo and R being various univalent ligands, such as CR′$_3$, NR′$_2$, OR′, SR′, and SeR′.[15] Despite several experimental attempts to characterize their heterodinuclear congeners, only the corresponding cation $[MoW(NMe_2)_6]^+$ could be observed by mass spectrometry, but not characterized structurally.[16] We consider only systems that have nonbridging ligands, excluding compounds such as $MoW(O_2CR_4)_4$, where bidentate ligands are bonded to both metals.[3]

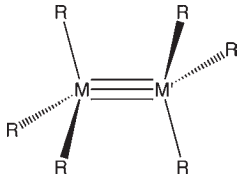


To shed light on the bonding situation of the electron-poor metal−metal triple bond and on terms that influence their stability and character, we set out a computational study of the homodinuclear and heterodinuclear systems $R_3M-M'R_3$ (M, M′ = Cr, Mo, W; R = Cl, $NMe_2$) (see Table 1), which may be classified as having a formal triple bond between two $d^3-MR_3$ fragments. Among the molecules in question, the homodimetallic molybdenum and tungsten compounds with $NMe_2$ ligands (i.e., $(NMe_2)_3Mo-Mo(NMe_2)_3$ and $(NMe_2)_3W-W(NMe_2)_3$) have been reported experimentally,[15c,h] and a theoretical interpretation was given in the early 1980s.[17] The chromium homologue is only known as the monometallic species $Cr(NMe_2)_3$.

This study is part of our ongoing work, the objective of which is systematic investigation of the chemical bond in transition-metal complexes,[18] with the help of energy decomposition analysis (EDA).[19−23] Our work is the first study where the $\sigma$ and $\pi$ contributions to the homodinuclear and heterodinuclear bonds of $R_3M-M'R_3$ are quantitatively evaluated.

## Computational Methods

All geometries were optimized at the gradient-corrected density functional theory (DFT) level of theory, using Becke's exchange functional,[24] in conjugation with Perdew's correlation functional[25] (BP86). Uncontracted Slater-type orbitals (STOs) were employed as basis functions in SCF calculations.[26] Triple-ζ-quality basis sets were used, which were augmented by two sets of polarization functions, that is *p* and *d* functions for the hydrogen atom, and *d* and *f* functions for the other atoms. This levels of theory is denoted as BP86/TZ2P. An auxiliary set of *s*, *p*, *d*, *f*, and *g* STOs was used to fit the molecular densities and represent the Coulombic and exchange potentials accurately in each SCF cycle.[27] Scalar relativistic effects were considered using the zero-order

(10) Braunstein, P.; Rose, J. *Comprehensive Organometallic Chemistry II: A Review of the Literature 1982−1994*, Vol. *10*; Abel, E. W., Stone, F. G. A., Wilkinson, G., Eds.; Pergamon Press: New York, 1995.
(11) Chetcuti, M. J. *Comprehensive Organometallic Chemistry II: A Review of the Literature 1982−1994*, Vol. *10*; Abel, E. W., Stone, F. G. A., Wilkinson, G., Eds.; Pergamon Press: New York, 1995.
(12) Gade, L. H. *Angew. Chem., Int. Ed.* **2000**, *39*, 2659.
(13) Wheatley, N.; Kalck, P. *Chem. Rev.* **1999**, *99*, 3379.
(14) Collmann, J. P.; Boulatov, R. *Angew. Chem., Int. Ed.* **2002**, *41*, 3948.
(15) (a) Chisholm, M. H.; Corning, J. F.; Folting, K.; Huffman, J. C. *Polyhedron* **1985**, *4*, 383. (b) Chisholm, M. H.; Parkin, I. P.; Huffman, J. C.; Streib, W. B. *J. Chem. Soc., Chem. Commun.* **1990**, 920. (c) Chisholm, M. H.; Cotton, F. A.; Frenz, B. A.; Reichert, W. W.; Shive, L. W.; Stults, B. R. *J. Am. Chem. Soc.* **1976**, *98*, 4469. (d) Chisholm, M. H.; Cotton, F. A.; Murillo, C. A.; Reichert, W. W. *Inorg. Chem.* **1977**, *16*, 1801. (e) Huq, F.; Mowat, W.; Shortland, A.; Skapski, A. C.; Wilkinson, G. *Chem. Commun.* **1971**, 1079. (f) Moawt, W.; Shortland, A.; Yagupski, G.; Hill, N. J.; Yagupsky, M.; Wilkinson, G. *J. Chem. Soc., Dalton Trans.* **1972**, 533. (g) Blatchford, T. P.; Chisholm, M. H.; Huffman, J. C. *Inorg. Chem.* **1987**, *26*, 1920. (h) Chisholm, M. H.; Cotton, F. A.; Extine, M.; Stults, B. R. *J. Am. Chem. Soc.* **1976**, *98*, 4477. (i) Chisholm, M. H.; Corning, J. F.; Huffman, J. C. *J. Am. Chem. Soc.* **1983**, *105*, 5924. (j) Chisholm, M. H.; Cotton, F. A.; Extine, M.; Stults, B. R. *Inorg. Chem.* **1976**, *15*, 2252. (k) Chisholm, M. H.; Folting, K.; Hampden-Smith, M.; Smith, C. A. *Polyhedron* **1987**, *6*, 1747. (l) Chisholm, M. H.; Clark, D. L.; Folting, K.; Huffman, J. C.; Hampden-Smith, M. *J. Am. Chem. Soc.* **1987**, *109*, 7750. (m) Alyea, E. C.; Basi, J. S.; Bradley, D. C.; Chisholm, M. H. *Chem. Commun.* **1968**, 495.
(16) Chisholm, M. H.; Extine, M. W.; Kelly, R. L.; Mills, W. C.; Murillo, C. A.; Rankel, L. A.; Reichert, W. W. *Inorg. Chem.* **1978**, *17*, 1673.
(17) Bursten, B. E.; Cotton, F. A.; Green, J. C.; Seddon, E. A.; Stanley, G. G. *J. Am. Chem. Soc.* **1980**, *102*, 4579.
(18) (a) Frenking, G.; Wichmann, K.; Fröhlich, N.; Loschen, C.; Lein, M.; Frunzke, J.; Rayón, V. M. *Coord. Chem. Rev.* **2003**, *55*, 238. (b) Lein, M.; Frenking, G. In *Theory and Applications of Computational Chemistry: The First 40 Years*; Dykstra, C. E., Frenking, G., Kim, K. S., Scuseria, G. E., Eds.; Elsevier: Amsterdam, 2005; p 367.
(19) Morokuma, K. *J. Chem. Phys.* **1971**, *55*, 1236.
(20) Kitaura, K.; Morokuma, K. *Int. J. Quantum Chem.* **1976**, *10*, 325.
(21) Bickelhaupt, F. M.; Baerends, E. J. *Rev. Comput. Chem.* **2000**, *15*, 1.
(22) Ziegler, T.; Rauk, A. *Theor. Chim. Acta* **1977**, *46*, 1.
(23) Ziegler, T.; Rauk, A. *Inorg. Chem.* **1979**, *18*, 1755.
(24) Becke, A. D. *Phys. Rev. A* **1988**, *38*, 3098.
(25) Perdew, J. P. *Phys. Rev. B* **1986**, *33*, 8822.
(26) Snijders, J. G.; Baerends, E. J.; Vernooijs, P. *At. Nucl. Data Tables* **1982**, *26*, 483.
(27) Krijn, J.; Baerends, E. J. *Fit Functions in the HFS Method* (in Dutch); *Internal Report*, Vrije Universiteit: Amsterdam, The Netherlands, **1984**.

regular approximation (ZORA).[28−32] Stationary points were characterized as minima on the potential energy surface by calculating the Hessian matrix analytically at this level. The energy decomposition analysis was also carried out at BP86/TZ2P. The calculations were performed using the ADF(2006) program package.[33] The natural bond orbital analysis (NBO) was carried out to calculate the atomic partial charges and the Wiberg bond orders using the Gaussian03 program package[34] at BP86 with split-valence basis sets of doubly polarized triple-ξ-quality developed by Weigend and Ahlrichs, which are denoted as def2-TZVPP.[35,36]

Complete Active Space (CAS) SCF[37] calculations have been carried out for homometallic $Cl_3MMCl_3$ molecules, to compare the results with the DFT calculations. The CASSCF calculations were then used to add dynamic correlation via multiconfigurational second-order perturbation theory (CASPT2).[38−40] Scalar relativistic effects were included via a Douglas−Kroll Hamiltonian.[41,42] Large ANO-RCC basis sets of Roos, such as those implemented in the program package MOLCAS,[43] were used in the following contractions: (17s12p5d4f2g) → [5s4p3d1f] for Cl, (21s15p10d6f4g2h) → [6s5p3d2f1g] for Cr, (21s18p13d6f4g2h) → [7s6p4d2f1g] for Mo (24s21p15d11f4g2h) → [8s7p5d3f1g] for W. These calculations were performed with the program MOLCAS6.[43] The CASPT2/ANO-RCC calculations were performed using BP86/TZ2P geometries. In the CASSCF calculations of the $Cl_3MMCl_3$ systems, we choose an active space that consists of 6 electrons in 10 orbitals CAS(6,10). We want to point out that a systematic comparison of the results that are obtained at BP86/TZ2P with CASPT2 calculations for a series of homonuclear and heteronuclear systems with a formal metal−metal quadruple bond $[MM'Cl_8]^x$ (M, M′ = Tc, Re, Ru, Os, Rh, Ir and $x$ = 2−, 1−, 0, 1+, 2+) has recently been published by us.[44] The agreement between the DFT and ab initio calculations is very good.

In the EDA, bond formation between the interacting fragments is divided into three steps, which can be interpreted in a plausible way. In the first step, the fragments, which are calculated with the frozen geometry of the entire molecule, are superimposed without electronic relaxation, yielding the quasiclassical electrostatic attraction ($\Delta E_{elstat}$). In the second step, the product wave function becomes antisymmetrized and renormalized, which gives the repulsive term ($\Delta E_{Pauli}$), termed Pauli repulsion. In the third step, the molecular orbitals relax to their final form to yield the stabilizing orbital interaction ($\Delta E_{orb}$). The latter term can be divided into contributions of orbitals having different symmetry. This latter step is crucial for the present study. The sum of the three terms $\Delta E_{elstat} + \Delta E_{Pauli} + \Delta E_{orb}$ gives the total interaction energy ($\Delta E_{int}$):

$$\Delta E_{int} = \Delta E_{elstat} + \Delta E_{Pauli} + \Delta E_{orb}$$

The EDA calculations, which involve open-shell fragments, do, for technical reasons, neglect the spin polarization in the fragments. This means that the interaction energies $\Delta E_{int}$ are slightly larger (on the order of a few kilocalories per mole per unpaired electron) than those using fully relaxed orbitals. This error has been neglected in the present study, because the small differences are unimportant for the discussion in this paper. To obtain the bond dissociation energy ($D_e$), the preparation energy ($\Delta E_{prep}$) must be considered, which is the energy difference of the fragments between their equilibrium geometry and the geometry that they have in the molecule.

$$\Delta E\ (= -D_e) = \Delta E_{int} + \Delta E_{prep}$$

Further details about the EDA can be found in the literature.[21,33]

Metal−metal bonded systems are considered to be multideterminantal problems. We have already reported that well-behaved systems such as those studied in this work can, at least for the purpose of bond analysis and for discussing stability and property trends, efficiently and reliably be described using DFT.[44,45]

## Results and Discussion

We begin the discussion with the $(NMe_2)_3M-M'(NMe_2)_3$ (M, M′ = Cr, Mo, W) molecules **1NMe$_2$−6NMe$_2$**. The molybdenum and tungsten compounds $(NMe_2)_3Mo-Mo(NMe_2)_3$ and $(NMe_2)_3W-W(NMe_2)_3$ are experimentally known and have been fully characterized,[15c,h] so that we can compare our computational with experimental data. The optimized geometrical parameters, the number of imaginary frequencies, the M−M′ bond dissociation energies, the NBO partial charges, and the Wiberg bond orders are summarized in Table 2.

All $(NMe_2)_3M-M'(NMe_2)_3$ molecules (**1NMe$_2$−6NMe$_2$**) adopt a staggered, $D_{3d}$ ($C_{3v}$ for heterodinuclear species)

(28) Chang, C.; Pelissier, M.; Durand, P. *Phys. Scr.* **1986**, *34*, 394.
(29) Heully, J. L.; Lindgren, I.; Lindroth, E.; Lundquist, S.; Martensson-Pendrill, A. M. *J. Phys. B* **1986**, *19*, 279.
(30) van Lenthe, E.; Baerends, E. J.; Snijders, J. G. *J. Chem. Phys.* **1993**, *99*, 4597.
(31) van Lenthe, E.; Baerends, E. J.; Snijders, J. G. *J. Chem. Phys.* **1996**, *105*, 6505.
(32) van Lenthe, E.; van Leeuwen, R.; Baerends, E. J.; Snijders, J. G. *Int. J. Quantum Chem.* **1996**, *57*, 281.
(33) te Velde, G.; Bickelhaupt, F. M.; Baerends, E. J.; van Gisbergen, S. J. A.; Fonseca Guerra, C.; Snijders, J. G.; Ziegler, T. *J. Comput. Chem.* **2001**, *22*, 931.
(34) Frisch, M. J.; Trucks, G. W.; Schlegel, H. B.; Scuseria, G. E.; Robb, M. A.; Cheeseman, J. R.; Montgomery Jr, J. A.; Vreven, J.; Kudin, K. N.; Burant, J. C.; Millam, J. M.; Iyengar, S. S.; Tomasi, J.; Barone, V.; Mennucci, B.; Cossi, M.; Scalmani, G.; Rega, N.; Petersson, G. A.; Nakatsuji, H.; Hada, M.; Ehara, M.; Toyota, K.; Fukuda, R.; Hasegawa, J.; Ishida, M.; Nakajima, T.; Honda, Y.; Kitai, O.; Nakai, H.; Klene, M.; Li, X.; Knox, E.; Hratchian, H. P.; Cross, J. B.; Bakken, V.; Adamo, C.; Jaramillo, J.; Gomperts, R.; Stratmann, R. E.; Yazyev, O.; Austin, A. J.; Cammi, R.; Pomelli, C.; Ochterski, J. W.; Ayala, P. Y.; Morokuma, K.; Voth, G. A.; Salvador, P.; Dannenberg, J. J.; Zakrzewski, V. G.; Dapprich, S.; Daniels, A. D.; Strain, M. C.; Farkas, O.; Malick, D. K.; Rabuck, A. D.; Raghavachari, K.; Foresman, J. B.; Ortiz, J. V.; Cui, Q.; Baboul, A. G.; Clifford, S.; Cioslowski, J.; Stefanov, B. B.; Liu, G.; Liashenko, A.; Piskorz, P.; Komaromi, I.; Martin, R. L.; Fox, D. J.; Keith, T.; Al-Laham, M. A.; Peng, C. Y.; Nanayakkara, A.; Challacombe, M.; Gill, P. M. W.; Johnson, B.; Chen, W.; Wong, M. W.; Gonzalez, C.; Pople, J. A. Gaussian 03 (Revision D.01); Gaussian, Inc.: Wallingford, CT, **2004**.
(35) Weigend, F.; Ahlrichs, R. *Phys. Chem. Chem. Phys.* **2005**, *7*, 3297.
(36) Weigend, F. *Phys. Chem. Chem. Phys.* **2006**, *8*, 1057.
(37) Roos, B. O. In *Advances in Chemical Physics; Ab initio Methods in Quantum Chemistry—II*; Lawley, K. P., Ed.; John Wiley & Sons Ltd.: Chichester, U.K., 1987; p 399.
(38) Andersson, K.; Malmqvist, P.-Å.; Roos, B. O.; Sadlej, A. J.; Wolinski, K. *J. Phys. Chem.* **1990**, *94*, 5483.
(39) Andersson, K.; Malmqvist, P.-Å.; Roos, B. O. *J. Chem. Phys.* **1992**, *96*, 1218.
(40) Roos, B. O.; Andersson, K.; Fülscher, M. P.; Malmqvist, P.-Å.; Serrano-Andrés, L.; Pierloot, K.; Merchán, M. In *Advances in Chemical Physics: New Methods in Computational Quantum Mechanics*, Vol. *XCIII*; Prigogine, I., Rice, S. A., Eds.; Wiley: New York, 1996; p 219.
(41) Douglas, N.; Kroll, N. M. *Ann. Phys.* **1974**, *82*, 89.
(42) Hess, B. *Phys. Rev. A* **1986**, *33*, 33742.
(43) Karlström, G.; Lindh, R.; Malmqvist, P.-Å.; Roos, B. O.; Ryde, U.; Veryazov, V.; Widmark, P.-O.; Cossi, M.; Schimmelpfennig, B.; Neograday, P.; Seijo, L. *Comput. Mater. Sci.* **2003**, *28*, 222.
(44) Takagi, N.; Krapp, A.; Frenking, G. *Can. J. Chem.* **2010**, *88*, 1079.
(45) Krapp, A.; Lein, M.; Frenking, G. *Theor. Chem. Acc.* **2008**, *120*, 313.

**Table 2.** Calculated Bond Lengths ($R$(M−M′)), Bond Angles ($A$(M−M′−N) and $A$(M′−M−Cl)), Number of Imaginary Frequencies (Nimag), Bond Dissociation Energies ($D_e$) of the M−M′ Bond, NBO Partial Charges ($q$), and Wiberg Bond Orders ($P$(M−M′)) of Compounds **1NMe$_2$**−**6NMe$_2$** with Staggered $D_{3d}$ ($C_{3v}$ for Heteronuclear Molecules) Symmetry at the BP86/TZ2P Level

| compound | **1NMe$_2$** (Cr−Cr) | **2NMe$_2$** (Mo−Mo) | **3NMe$_2$** (W−W) | **4NMe$_2$** (Cr−Mo) | **5NMe$_2$** (Cr−W) | **6NMe$_2$** (Mo−W) |
|---|---|---|---|---|---|---|
| $R$(M−M′) | 1.892 Å | 2.232 Å | 2.318 Å | 2.069 Å | 2.130 Å | 2.279 Å |
| $A$(M−M′−N) | 105.3° | 103.9° | 103.8° | 105.2° | 104.7° | 104.0° |
| $A$(M′−M−N) | 105.3° | 103.9° | 103.8° | 103.9° | 103.7° | 103.5° |
| Nimag | 0 | 0 | 0 | 0 | 0 | 0 |
| $D_e$ | 25.9 kcal/mol | 85.4 kcal/mol | 103.6 kcal/mol | 54.0 kcal/mol | 60.8 kcal/mol | 94.1 kcal/mol |
| $q$(M) | 0.66 $e$ | 0.86 $e$ | 1.02 $e$ | 0.40 $e$ | 0.23 $e$ | 0.74 $e$ |
| $q$(M′) | 0.66 $e$ | 0.86 $e$ | 1.02 $e$ | 1.05 $e$ | 1.41 $e$ | 1.11 $e$ |
| $q$((NMe$_2$)$_3$M) | 0.00 $e$ | 0.00 $e$ | 0.00 $e$ | −0.25 $e$ | −0.42 $e$ | −0.12 $e$ |
| $P$(M−M′) | 2.11 | 2.26 | 2.26 | 2.14 | 2.11 | 2.24 |
| $E_{rel}$[a] | 26.8 | 26.9 | 25.6 | 26.2 | 25.1 | 26.2 |

[a] Relative energies between staggered and eclipsed structures, given in units of kcal/mol.

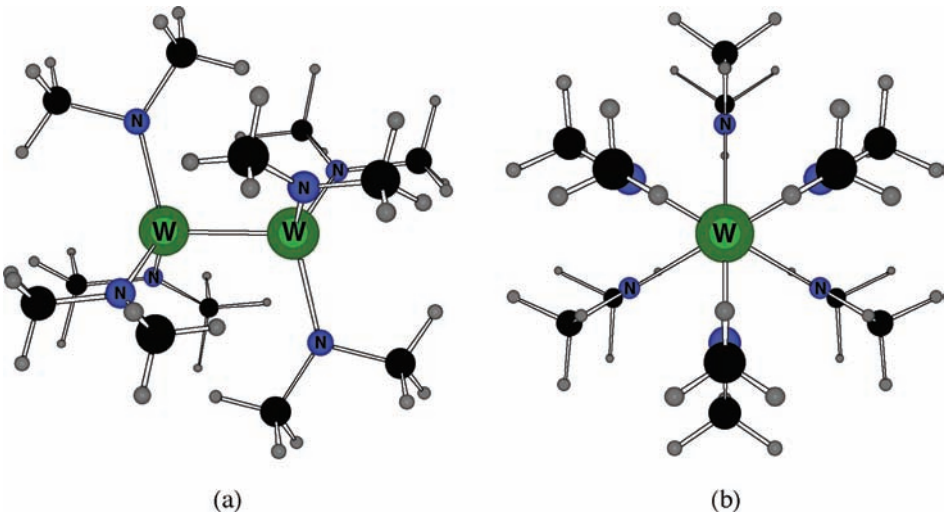


**Figure 1.** Optimized $D_{3d}$ symmetric geometry of **3NMe$_2$** from (a) side view and (b) top view at the BP86/TZ2P level.

conformation of the two M(NMe$_2$)$_3$ units. The eclipsed $D_{3d}$ ($C_{3h}$) structures do not correspond to minima on the potential energy surface, and they are less stable, by 25.1−26.9 kcal/mol, with respect to the staggered ones, according to constraint geometry optimizations. This observation agrees with the experimental X-ray structures of (NMe$_2$)$_3$Mo−Mo(NMe$_2$)$_3$ and (NMe$_2$)$_3$W−W(NMe$_2$)$_3$, because only the staggered conformers exist in the crystals. The optimized M−M′ distances for **2NMe$_2$** (2.232 Å) and **3NMe$_2$** (2.318 Å) reproduce those from the X-ray structures of 2.214 Å and 2.292 Å, respectively, well. Also, the remaining structural features of the optimized **2NMe$_2$** and **3NMe$_2$** agree very well with the experimentally reported ones,[15c,h] which makes us confident that the current computational method is reliable for the purpose of this study.

As shown in Figure 1, the N−C−C plane in the NMe$_2$ ligands of **1NMe$_2$**−**6NMe$_2$** lies always parallel to the central M−M′−N plane. In a recent work on the bonding in early-late complexes,[46] we observed a rather strong dependency of the M−M′ bond length on the orientation of NR$_2$ ligands. This could be explained by the lone-pair orbitals on the amino groups mixing into the M−M′ $\sigma$-orbital. Although, following the conclusions in ref 46, a 90° rotation of the NMe$_2$ groups is expected to strengthen (and lengthen) the M−M′ bond, such conformers become energetically unfavorable in the present case, by more than 90 kcal/mol, and do not correspond to minima on the potential energy hypersurface. Therefore, in the following, we will consider only the $D_{3d}$ ($C_{3v}$) symmetric structures, as illustrated in Figure 1.

The optimized M−M′ distances in **1NMe$_2$**−**6NMe$_2$** are all considerably shorter than the sum of their van der Waals radii, indicating multiple bond character of the M−M′ bonds. As expected, the M−M′ distance increases for heavier M and M′. In the heterodinuclear compounds, the M−M′ bond lengths are very close to the geometrical mean of the corresponding homodinuclear M−M values, only for **5NMe$_2$**, the optimized value of 2.130 Å is slightly larger than the geometrical mean of **1NMe$_2$** and **3NMe$_2$** of 2.105 Å.

The bond strength increases significantly as M and M′ become heavier, as indicated by the bond dissociation energy ($D_e$). $D_e$ increases in the order of **1NMe$_2$** (25.0 kcal/mol) < **2NMe$_2$** (85.7 kcal/mol) < **3NMe$_2$** (103.6 kcal/mol) for the homodinuclear molecules. We want to note that the chromium compound **1NMe$_2$** has a much weaker bond than the molybdenum and tungsten homologues. This is consistent with the experimental finding that (NMe$_2$)$_3$Mo−Mo(NMe$_2$)$_3$ and (NMe$_2$)$_3$W−W(NMe$_2$)$_3$ are experimentally known[15c,h] but the chromium species is only known as monomer (NMe$_2$)$_3$Cr.[15m] If thermal and entropic corrections are considered for the bond dissociation energy, the molecule (NMe$_2$)$_3$Cr−Cr(NMe$_2$)$_3$ is only weakly bonded. The experimental observations suggest that the intramolecular interactions provide sufficient stability to the monomer (NMe$_2$)$_3$Cr, preventing the formation of **1NMe$_2$** in a condensed phase.

(46) Krapp, A.; Frenking, G. *Theor. Chem. Acc.* **2010**, *127*, 141.

**Table 3.** EDA for Compounds $\mathbf{1NMe_2}$–$\mathbf{6NMe_2}$ at the BP86/TZ2P Level under $C_{3v}$ Symmetry[a]

| compound | $\mathbf{1NMe_2}$ (Cr−Cr) | $\mathbf{2NMe_2}$ (Mo−Mo) | $\mathbf{3NMe_2}$ (W−W) | $\mathbf{4NMe_2}$ (Cr−Mo) | $\mathbf{5NMe_2}$ (Cr−W) | $\mathbf{6NMe_2}$ (Mo−W) |
|---|---|---|---|---|---|---|
| $\Delta E_{int}$ (kcal/mol) | −61.6 | −108.7 | −127.5 | −83.1 | −89.7 | −117.6 |
| $\Delta E_{Pauli}$ (kcal/mol) | 367.2 | 418.1 | 447.4 | 386.1 | 386.6 | 429.4 |
| $\Delta E_{elstat}$[b] (kcal/mol) | −242.2 (56.5%) | −326.9 (62.1%) | −377.5 (65.7%) | −279.7 (59.6%) | −293.7 (61.7%) | −349.9 (64.0%) |
| $\Delta E_{orb}$ (kcal/mol)[b] | −186.7 (43.5%) | −199.9 (37.9%) | −197.5 (34.4%) | −189.5 (40.4%) | −182.6 (38.4%) | −197.2 (36.1%) |
| $a_1$ ($\sigma$)[c] | −68.2 (36.5%) | −71.1 (35.6%) | −69.4 (35.1%) | −69.1 (36.5%) | −66.6 (36.5%) | −69.5 (35.2%) |
| $a_2$[c] | −0.9 (0.5%) | −0.6 (0.3%) | −0.5 (0.3%) | −0.7 (0.4%) | −0.7 (0.4%) | −0.5 (0.3%) |
| $e$ ($\pi$)[c] | −117.6 (63.0%) | −128.2 (64.2%) | −127.6 (64.6%) | −119.7 (63.2%) | −115.3 (63.2%) | −127.2 (64.5%) |
| $\Delta E_{prep}$ (kcal/mol) | 36.6 | 23.0 | 23.9 | 29.3 | 28.3 | 23.4 |
| $-D_e$ (kcal/mol) | 25.0 | 85.7 | 103.6 | 53.8 | 60.4 | 94.2 |

[a] The respective quartet $^4A_1$ state was chosen for the interacting fragments $M(NMe_2)_3$. [b] The percentage values given in parentheses represent the contribution to the total attractive interactions $\Delta E_{elstat} + \Delta E_{orb}$. [c] The percentage values given in parentheses represent the contribution to the total orbital interactions $\Delta E_{orb}$.

The trend for the bond strengths of the heterodinuclear compounds is $\mathbf{4NMe_2}$ (53.8 kcal/mol) < $\mathbf{5NMe_2}$ (60.4 kcal/mol) < $\mathbf{6NMe_2}$ (94.2 kcal/mol). The strongest M-M′ bond is predicted for the heaviest compound $\mathbf{3NMe_2}$ in which two 5*d* metals are bound together. We note that the experimental difficulties in the synthesis of heterodinuclear species and especially also $\mathbf{6NMe_2}$ are not due to the intrinsic instability of the polar M−M′ bonds. All heterodinuclear compounds $\mathbf{4NMe_2}$–$\mathbf{6NMe_2}$ are predicted to be thermodynamically sufficiently stable, with respect to decomposition to $M(NMe_2)_3$ fragments, to allow for an experimental observation, once a synthetic path has been found. The decomposition of two heterodinuclear species into the homodinuclear compounds is almost thermoneutral, and careful low-temperature experiments should allow the isolation of the heterodinuclear species $\mathbf{4NMe_2}$–$\mathbf{6NMe_2}$.

The bond strength of the heterodinuclear compounds corresponds almost exactly to the geometrical mean of the corresponding homodinuclear compounds. This indicates a very similar bonding situation in both the homodinuclear and heterodinuclear systems, with the bond polarity in the heterodinuclear species being either small or without effect on the structural parameters and the bond strengths.

For the relaxed $d^3$-$M(NMe_2)_3$ fragments, we considered two electronic structures: a quartet and a doublet state. The trigonal planar quartet state ($^4A_1$) corresponds to the electronic ground state for all $M(NMe_2)_3$ fragments. In the W-$(NMe_2)_3$ fragment, the terminal $NMe_2$ groups lie exactly perpendicular to the central N−W−N plane, suggesting $C_{3v}$ symmetry, whereas they are rotated along the M−N axis (24°−27°) for $Cr(NMe_2)_3$ and $Mo(NMe_2)_3$, which adopt $C_3$ symmetry. The trigonal pyramidal doublet states ($^2A_1$) correspond to the electronic excited state. The excitation energies $^4A_1 \rightarrow {}^2A_1$ are calculated to be 18.9, 10.6, and 3.8 kcal/mol for $Cr(NMe_2)_3$, $Mo(NMe_2)_3$, and $W(NMe_2)_3$, respectively.

The NBO analysis shows that the metal atoms carry a relatively large positive charge, because of the strong electronegative $NMe_2$ ligands. For the homodinuclear molecules, the positive charges of M increase in the following order: $\mathbf{1NMe_2}$ (0.66 *e*) < $\mathbf{2NMe_2}$ (0.86 *e*) < $\mathbf{3NMe_2}$ (1.02 *e*). The largest bond polarity in the heterodimetallic systems, as measured by the charge of the $M(NMe_2)_3$ units, is predicted for the 3*d*−5*d* system $\mathbf{5NMe_2}$. The charge transferred from $W(NMe_2)_3$ to $Cr(NMe_2)_3$ amounts to 0.4 *e*. The charge transfer in $\mathbf{4NMe_2}$ and $\mathbf{6NMe_2}$ is 0.3 *e* and 0.1 *e*. In all heterodinuclear systems, the polarity is such that charge is transferred from the heavier metal to the lighter metal.

Interestingly, note that the Wiberg bond index $P(M-M')$, as an indicator of the covalency of the M−M′ bond, is almost constant, ∼2.1−2.2 for the entire set of $(Me_2N)_3M-M'(NMe_2)_3$ systems considered, meaning that one could assign a triple bond character to all of these M−M′ bonds. Furthermore, this can be seen as an indication that the covalent part of the M−M′ bonds has similar character and strength, whereas the substantial difference in bond strength ($D_e$) must be mainly a result of the change in the electrostatic contribution to the bond energy. The results of the energy decomposition analysis (EDA) for $\mathbf{1NMe_2}$–$\mathbf{6NMe_2}$, as presented in Table 3, will shed light on this hypothesis.

The respective $^4A_1$ quartet states for the neutral $(NMe_2)_3M$ and $M'(NMe_2)_3$ fragments were chosen as the interacting moieties in the EDA. The interaction energy ($\Delta E_{int}$) follows the same trend as the dissociation energy ($D_e$). The observation that the values for the heterodinuclear species almost match the geometrical mean of the homodinuclear congeners also holds for the interaction energies. This means that one can disregard the deformation of the fragments, as measured by the preparation energy, to explain the increase in the dissociation energy with increasing mass of the metal M. There are two important observations to be made when considering the stabilizing contributions to the interaction energy ($\Delta E_{elstat} + \Delta E_{orb}$). First, they are dominated by the electrostatic contribution $\Delta E_{elstat}$, which amounts to 57% of the total stabilizing contributions ($\Delta E_{elstat} + \Delta E_{orb}$) in $\mathbf{1NMe_2}$, 62% in $\mathbf{2NMe_2}$, 66% in $\mathbf{3NMe_2}$, 60% in $\mathbf{4NMe_2}$, 62% in $\mathbf{5NMe_2}$, and 64% in $\mathbf{6NMe_2}$. Second, the absolute value of the orbital term is very similar for $\mathbf{1NMe_2}$–$\mathbf{6NMe_2}$, because it only varies between −183 kcal/mol and −200 kcal/mol, compared to the variation in $\Delta E_{elstat}$ (between −242.2 kcal/mol and −377.5 kcal/mol). Also taking into account that the repulsive Pauli term ($\Delta E_{Pauli}$) varies relatively little, we conclude that the increase in the stability of the M−M′ bond when going to heavier metal atoms M and M′ is due to an increase in the quasiclassical attraction of the $M(NMe_2)_3$ and $M'(NMe_2)_3$ fragments. The lower electrostatic contributions for the lighter metal atoms can be explained by the more-compact valence orbitals of the lighter metal atoms and their smaller positive partial charge, which is due to a decrease in N−M bond polarity.

The covalent bonding, as measured by the orbital relaxation contribution $\Delta E_{orb}$, is relatively constant, which corroborates the finding of the Wiberg bond orders. The orbital contributions can be split up in components of $a_1$, $a_2$, and *e* character. The $a_2$-symmetric contributions are negligibly small, whereas the $a_1$- and *e*-symmetric contributions can

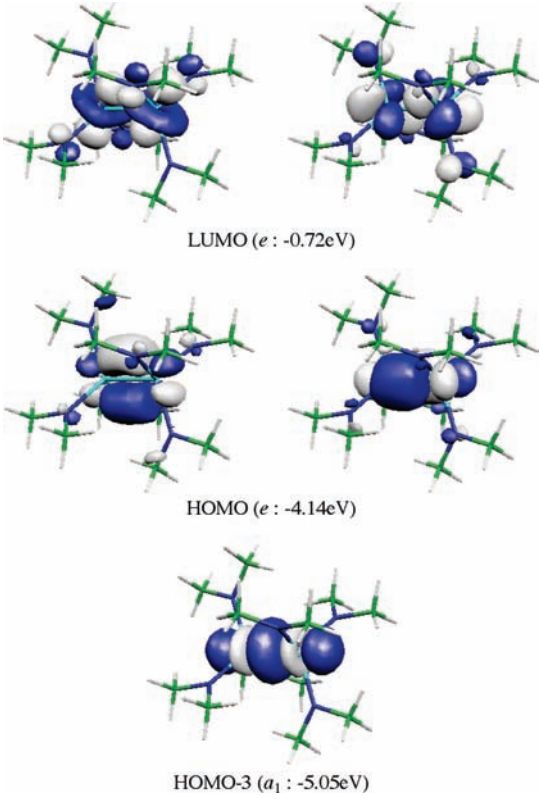


**Figure 2.** Plot of relevant orbitals and eigenvalues of **3NMe$_2$** at the BP86/TZ2P level.

be identified as the M−M′−$\sigma$- and M−M′−$\pi$-bonding contributions, respectively. The numerical values of the $a_1(\sigma)$ and $e(\pi)$ components for **1NMe$_2$**−**6NMe$_2$** show that the M−M′ bonds consist consistently of one $\sigma$-bond, which contributes ∼36% to the total orbital relaxation energy, and two $\pi$-bonds of almost equal importance as the $\sigma$-bond (2 × 32%). We note that the heterodinuclear compounds **4NMe$_2$**−**6NMe$_2$** exhibit very similar behavior in the EDA as their homodinuclear counterparts, as expected from the charge analysis. The individual energy contributions to the interaction energy for the heterodinuclear systems are between the respective values of the homodinuclear compounds, except for the electrostatic contribution $\Delta E_{\text{elstat}}$ in **5NMe$_2$** and **6NMe$_2$**, where it is slightly smaller. It seems that the small charge transfer between the different metal atoms remains without major effects on the bonding situation.

The Kohn−Sham orbital pictures of **1NMe$_2$**−**6NMe$_2$**, as shown in Figure 2, allow for a visualization of the M−M′−$\sigma$- and −$\pi$-bonds. Interestingly, note that **1NMe$_2$**−**6NMe$_2$** have energetically lower-lying degenerated lowest unoccupied molecular orbitals (LUMOs), which correspond to metal−metal $\delta$-bonds and $\delta$*-bonds. The LUMO energies increase in the following orders: for the homonuclear molecules, **1NMe$_2$** (−1.81 eV) < **2NMe$_2$** (−1.22 eV) < **3NMe$_2$** (−0.72 eV); for the heteronuclear molecules,**4NMe$_2$** (−1.53 eV) < **5NMe$_2$** (−1.33 eV) < **6NMe$_2$** (−0.97 eV). Anionic states of **1NMe$_2$** under $D_{3h}$ symmetry constraint have much shorter M−M′ distances (1.808 Å at the dianionic singlet state, and 1.819 Å at the dianionic triplet state). The latter is more stable than the former by 8.5 kcal/mol. They clearly have short Cr−Cr bonds, comparable to the recently reported molecules, which have very short Cr−Cr bonds (1.740−1.823 Å).[4−9]

The results of the model molecules $R_3M-M'R_3$, where R = Cl (**1Cl**−**6Cl**), are presented in Tables 4 and 5. We considered two possible conformers: the staggered structures **1Cl**−**6Cl** and the eclipsed structures **1Cl′**−**6Cl′**. The calculations show that the staggered structures are the most favorable ones among the isomers that have direct M−M′ bonds, except for **3Cl**, which has a small imaginary frequency ($6.1i$ cm$^{-1}$), whose vector is pointing toward the corresponding eclipsed structure. However, for all $Cl_3M-M'Cl_3$ molecules, the energy differences between the staggered and the eclipsed structure are small, with a preference for the staggered structure for all species but $Cl_3W-WCl_3$. The small energy differences come from weak repulsion between the chlorine ligands, as indicated by the slightly longer M−M′ distances, and the tilted bond angles of M−M′−Cl and M′−M−Cl for **1Cl′**−**6Cl′**. In the following, for the sake of simplicity, we will mainly discuss the staggered structures **1Cl**−**6Cl**.

The central M−M′ bonds in **1Cl**−**6Cl** are almost equally long, compared to **1NMe$_2$**−**6NMe$_2$**, except for the chromium compound **1Cl**, which has a 0.03-Å-longer Cr−Cr bond than **1NMe$_2$**.

The bond dissociation energies ($D_e$) of **1Cl**−**6Cl** follow the same trends as in **1NMe$_2$**−**6NMe$_2$**. Also, in this case, a heavier metal leads to stronger M−M′ bonds. Hence, the strongest M−M′ bond is predicted for the (5*d*−5*d*) compound **3Cl** with $D_e$ = 99.8 kcal/mol. The change of ligands R in $R_3M-M'R_3$ from R = $NMe_2$ to R = Cl leads to destabilization of the metal−metal bond. This is most pronounced for the lighter systems with M = Cr.

The NBO analysis shows that the metal atoms M and M′ in **1Cl**−**6Cl** always carry a positive charge, but much less so than the metal atoms in **1NMe$_2$**−**6NMe$_2$**. However, the amount of charge transfer and, thereby, the polarity of the metal−metal bond in the heterodinuclear compounds is very similar for both classes of compounds with ligands R = Cl and R = $NMe_2$. Also, the Wiberg bond orders remain almost unchanged by the change of ligand in $R_3M-M'R_3$. Based on the charge analysis, we expect the M−M′ bond in **1Cl**−**6Cl** to have a similar degree of covalency, but a reduced quasiclassical electrostatic contribution, because of the less-positive character of the metal atoms.

For detailed analysis of the M−M′ bonding situation, the EDA is carried out for **1Cl**−**6Cl**. The respective quartet $^4A_1$ states were chosen as the interacting moieties for the $Cl_3M$ and $M'Cl_3$ fragments. The EDA results are summarized in Table 5. The EDA shows that the $\Delta E_{\text{int}}$ values increase as the metal atoms become heavier in the following order: for the homodinuclear molecules, **1Cl** (−29.9 kcal/mol) < **2Cl** (−90.2 kcal/mol) < **3Cl** (−115.8 kcal/mol); for the heterodinuclear molecules, **4Cl** (−60.5 kcal/mol) < **5Cl** (−71.9 kcal/mol) < **6Cl** (−102.7 kcal/mol). As for **1NMe$_2$**−**6NMe$_2$**, the behavior of $\Delta E_{\text{int}}$ closely resembles that of $D_e$, because all molecules have similar $\Delta E_{\text{prep}}$ values of 13.1−17.8 kcal/mol. When it comes to the individual contributions to the interaction energy, we note the general similarity to the amino systems **1NMe$_2$**−**6NMe$_2$**. The EDA supports the above statement that the covalent contribution is very much the same for the chloride and the amino compounds, both exhibiting triple bonds with a slightly dominating $\sigma$-bond contribution and a degenerate $\pi$-contribution. In **1Cl**−**6Cl**, the amount of $\pi$-bonding is slightly reduced and the amount of $\sigma$-bonding is slightly increased, compared to **1NMe$_2$**−**6NMe$_2$**. The EDA also gives an explanation for

**Table 4.** Calculated Bond Lengths ($R$(M−M′)), Bond Angles ($A$(M−M′−Cl) and $A$(M′−M−Cl)), Number of Imaginary Frequencies (Nimag), Bond Dissociation Energies ($D_e$) of the M−M′ Bond, NBO Partial Charges ($q$), and Wiberg Bond Orders ($P$(M−M′)) of Compounds **1Cl**−**6Cl** with Staggered-$D_{3d}$ ($C_{3v}$ for Heteronuclear Molecules) and **1Cl′**−**6Cl′** with Eclipsed-$D_{3h}$ ($C_{3h}$ for Heteronuclear Molecules) Symmetry at the BP86/TZ2P Level[a]

| | | | Staggered | | | |
|---|---|---|---|---|---|---|
| compound | **1Cl** (Cr−Cr) | **2Cl** (Mo−Mo) | **3Cl** (W−W) | **4Cl** (Cr−Mo) | **5Cl** (Cr−W) | **6Cl** (Mo−W) |
| $R$(M−M′) | 1.926 Å | 2.228 Å | 2.308 Å | 2.078 Å | 2.128 Å | 2.271 Å |
| $A$(M−M′−Cl) | 105.0° | 102.8° | 103.2° | 105.5° | 105.0° | 103.3° |
| $A$(M′−M−Cl) | 105.0° | 102.8° | 103.2° | 101.9° | 101.5° | 102.5° |
| Nimag | 0 | 0 | 1 (6.1$i$ cm$^{-1}$) | 0 | 0 | 0 |
| $D_e$ | 12.1 kcal/mol | 77.1 kcal/mol | 99.8 kcal/mol | 44.8 kcal/mol | 54.9 kcal/mol | 88.2 kcal/mol |
| $q$(M) | 0.32 $e$ | 0.53 $e$ | 0.65 $e$ | 0.16 $e$ | 0.06 $e$ | 0.47 $e$ |
| $q$(M′) | 0.32 $e$ | 0.53 $e$ | 0.65 $e$ | 0.72 $e$ | 0.93 $e$ | 0.73 $e$ |
| $q$($Cl_3$M) | 0.00 $e$ | 0.00 $e$ | 0.00 $e$ | −0.24 $e$ | −0.39 $e$ | −0.13 $e$ |
| $P$(M−M′) | 2.12 | 2.20 | 2.26 | 2.13 | 2.12 | 2.23 |
| | | | Eclipsed | | | |
| compound | **1Cl′** (Cr−Cr) | **2Cl′** (Mo−Mo) | **3Cl′** (W−W) | **4Cl′** (Cr−Mo) | **5Cl′** (Cr−W) | **6Cl′** (Mo−W) |
| $R$(M−M′) | 1.990 | 2.267 | 2.337 | 2.130 | 2.178 | 2.305 |
| $A$(M−M′−Cl) | 106.9° | 103.8° | 103.5° | 105.0° | 104.4° | 103.6° |
| $A$(M′−M−Cl) | 106.9° | 103.8° | 103.5° | 105.6° | 105.4° | 103.5° |
| Nimag | 0 | 1 (5.9$i$ cm$^{-1}$) | 0 | 1 (21.1$i$ cm$^{-1}$) | 1 (20.3$i$ cm$^{-1}$) | 0 |
| $D_e$ | 7.9 kcal/mol | 76.2 kcal/mol | 100.1 kcal/mol | 41.6 kcal/mol | 52.0 kcal/mol | 87.9 kcal/mol |
| $q$(M) | 0.29 $e$ | 0.49 $e$ | 0.62 $e$ | 0.11 $e$ | 0.03 $e$ | 0.43 $e$ |
| $q$(M′) | 0.29 $e$ | 0.49 $e$ | 0.62 $e$ | 0.70 $e$ | 0.89 $e$ | 0.70 $e$ |
| $q$($Cl_3$M) | 0.00 $e$ | 0.00 $e$ | 0.00 $e$ | −0.24 $e$ | −0.38 $e$ | −0.14 $e$ |
| $P$(M−M′) | 1.99 | 2.09 | 2.19 | 2.02 | 2.03 | 2.14 |
| $E_{rel}$[a] | +4.2 | +0.8 | −0.2 | +3.2 | +2.9 | +0.3 |

[a] Relative energies between staggered and eclipsed structures, given in units of kcal/mol.

**Table 5.** EDA Results for Compounds **1Cl**−**6Cl** at the BP86/TZ2P Level under $C_{3v}$ Symmetry[a]

| compound | **1Cl** (Cr−Cr) | **2Cl** (Mo−Mo) | **3Cl** (W−W) | **4Cl** (Cr−Mo) | **5Cl** (Cr−W) | **6Cl** (Mo−W) |
|---|---|---|---|---|---|---|
| $\Delta E_{int}$ (kcal/mol) | −29.9 | −90.2 | −115.8 | −60.5 | −71.9 | −102.7 |
| $\Delta E_{Pauli}$ (kcal/mol) | 249.5 | 320.3 | 371.2 | 287.4 | 304.1 | 342.3 |
| $\Delta E_{elstat}$[b] (kcal/mol) | −120.5 (43.1%) | −216.8 (52.8%) | −289.3 (59.4%) | −170.9 (49.1%) | −198.5 (52.8%) | −249.7 (56.1%) |
| $\Delta E_{orb}$[b] (kcal/mol) | −158.9 (56.9%) | −193.8 (47.2%) | −197.7 (40.6%) | −177.0 (50.9%) | −177.5 (47.2%) | −195.3 (43.9%) |
| $a_1$ ($\sigma$)[c] | −65.5 (41.2%) | −74.6 (38.5%) | −75.5 (38.2%) | −70.5 (39.8%) | −71.3 (40.2%) | −75.0 (38.4%) |
| $a_2$[c] | −0.1 (0.1%) | −0.1 (0.0%) | −0.1 (0.0%) | −0.1 (0.1%) | −0.1 (0.1%) | −0.1 (0.0%) |
| $e$ ($\pi$)[c] | −93.3 (58.7%) | −119.1 (61.5%) | −122.1 (61.8%) | −106.4 (60.1%) | −106.2 (59.8%) | −120.3 (61.6%) |
| $\Delta E_{prep}$ (kcal/mol) | 17.8 | 13.1 | 16.0 | 15.7 | 17.0 | 14.5 |
| $-D_e$ | 12.1 | 77.1 | 99.8 | 44.8 | 54.9 | 88.2 |

[a] The respective quartet $^4A_1$ state was chosen for the interacting fragments $MCl_3$. [b] The percentage values in parentheses give the contribution to the total attractive interactions $\Delta E_{elstat} + \Delta E_{orb}$. [c] The percentage values in parentheses give the contribution to the total orbital interactions $\Delta E_{orb}$.

the reduced stability of the chloride systems, compared to the amino systems. The absolute value of the stabilizing electrostatic contribution $\Delta E_{elstat}$ is reduced rather drastically in **1Cl**−**6Cl**, compared to **1NMe$_2$**−**6NMe$_2$**. This can be explained by the reduced positive charge of the metal atoms in the chloride compounds, as revealed by the charge analysis, because this leads to an effective screening of the nuclear charge of the metal atoms, thereby reducing the net attraction of the electrons from one fragment by the metal nucleus of the other fragment.

We carried out additional CASPT2 calculations for the homometallic systems $Cl_3MMCl_3$, to check whether the conclusions that were made using DFT data might change when multireference ab initio calculations are employed. It has previously been shown in numerous studies by Gagliardi and Roos[47] that compounds with metal−metal multiple bonds are well-described using CASPT2. We want to point out that our recent work on formally quadruply bonded systems with the general formula $[MM'Cl_8]^x$ (M, M′ = Tc, Re, Ru, Os, Rh, Ir and $x$ = 2−, 1−, 0, 1+, 2+) showed that DFT performs quite well, in comparison with CASPT2.[44]

Table 6 shows the calculated bond dissociation energies (BDEs) and the occupation of the bonding and antibonding $\sigma$- and $\pi$-orbitals, as well as the bond order at CASPT2 for the homoatomic systems **1Cl**, **2Cl**, and **3Cl**. The theoretically predicted BDEs at CASPT2 are, in all cases, ∼5 kcal/mol smaller than the BP86 values; however, the relative values at the two levels of theory are very similar to each other. It is interesting to compare the EDA values for the $\sigma$- and $\pi$-interactions with the relative contributions of $\sigma$- and $\pi$ molecular orbitals to the orbital interactions in **1Cl**−**3Cl**, which is given by the effective occupation numbers

(47) (a) Brynda, M.; Gagliardi, L.; Roos, B. O. *Chem. Phys. Lett.* **2009**, *471*, 1. (b) Brynda, M.; Gagliardi, L.; Widmark, P.-O.; Power, P. P.; Roos, B. O. *Angew. Chem., Int. Ed.* **2006**, *45*, 3804. (c) Roos, B. O.; Borin, A.; Gagliardi, L. *Angew. Chem., Int. Ed.* **2007**, *46*(9), p1469–1472. (d) Gagliardi, L. In *Reviews in Computational Chemistry*, Vol. *25*; Lipkowitz. K. B., Cundari. T. R., Eds.; John Wiley & Sons, Inc.: Hoboken, NJ, 2007; pp 249. (e) La Macchia, G.; Aquilante, F.; Veryazov, V.; Roos, B. O.; Gagliardi, L. *Inorg. Chem.* **2008**, *47*, 11455. (f) Gagliardi, L.; Roos, B. O. *Inorg. Chem.* **2003**, *42*, 1599.

**Table 6.** Orbital Occupation Numbers, Effective Bond Orders (BOs), and M−M′ Bond Dissociation Energies ($D_e$) of Compounds **1Cl**−**6Cl** at the CASPT2(6,10)/ANO-RCC Level Using BP86/TZ2P Optimized Geometries

| compound | **1Cl** (Cr−Cr) | **2Cl** (Mo−Mo) | **3Cl** (W−W) |
|---|---|---|---|
| Occ.($\pi$*) | 0.29, 0.30 | 0.13, 0.13 | 0.10, 0.10 |
| Occ.($\sigma$*) | 0.21 | 0.10 | 0.07 |
| Occ.($\pi$) | 1.70, 1.69 | 1.87, 1.87 | 1.89, 1.89 |
| Occ.($\sigma$) | 1.79 | 1.90 | 1.92 |
| $\sigma$(effective)[a] | 1.58 | 1.80 | 1.85 |
| $\pi$ (effective)[a] | 2.80 | 3.48 | 3.58 |
| BO[b] | 2.19 | 2.64 | 2.72 |
| $D_e$ (kcal/mol) | 7.4 | 73.1 | 94.0 |
| $D_e$ (kcal/mol)[c] | (12.1) | (77.1) | (99.8) |

[a] Calculated as differences of the $\sigma$ (Occ.($\sigma$) − Occ.($\sigma$*)) and $\pi$ (Occ.($\pi$) − Occ.($\pi$*)) MOs. [b] Denotes bond order, which is given by the sum of the effective occupation numbers $\sigma$(effective) and $\pi$ (effective) divided by 2, as suggested in ref 47f. [c] at BP86/TZ2P.

$\sigma$(effective) and $\pi$ (effective). The latter values are calculated as differences between the bonding and antibonding orbitals (Occ.($\sigma$) − Occ.($\sigma$*)) and (Occ.($\pi$) − Occ.($\pi$*)) in the CASPT2 calculations. The effective occupation numbers and the $\Delta E_{orb}$ values agree that the $\pi$-bonding is stronger than $\sigma$-bonding for the $Cl_3M-MCl_3$ interactions. This is gratifying, because the former values refer to the energy contribution to the covalent bonding, while the occupation numbers refer to the charge contribution. Table 6 also gives the bond orders (BOs), which have been suggested by Gaglidardi and Roos[47f] as a measure for the multiplicity of metal−metal bonding. The calculated BO is between 2.19 for the chromium compound and 2.72 for the tungsten compound, which can be interpreted as partial triple bond character.

## Summary and Conclusion

The metal−metal bonding situation in $R_3M-M'R_3$ (M, M′ = Cr, Mo, W; R = Cl, $NMe_2$) was investigated using density functional theory (DFT) calculations, with the help of energy decomposition analysis (EDA). The $R_3M-M'R_3$ compounds have short metal−metal bonds and prefer a staggered structure to prevent steric repulsion between facing ligands. The M−M′ bond strength increases as M and M′ become heavier. The strongest bond is predicted for the *5d*−*5d* tungsten complexes $(NMe_2)_3W-W(NMe_2)_3$ ($D_e$ = 103.6 kcal/mol) and $Cl_3W-WCl_3$ ($D_e$ = 99.8 kcal/mol). The properties and stabilities of heterodinuclear species are predicted to lie between the values for the respective homodinuclear species. The most-stable heterodinuclear M−M′ bond is predicted for $(NMe_2)_3Mo-W(NMe_2)_3$ ($D_e$ = 94.1 kcal/mol). The fact that the less-stable $(NMe_2)_3Mo-Mo(NMe_2)_3$ ($D_e$ = 85.4 kcal/mol) is experimentally known shows that the unsuccessful attempts to isolate $(NMe_2)_3Mo-W(NMe_2)_3$ are not due to an intrinsic thermodynamic instability of the compound. The charge analysis shows only moderate polarity of the M−M′ bond in the heterodimetallic species. The Wiberg bond order for all compounds is ∼2.1, which indicates triple bond character of the M−M′ bonds.

The EDA results show that electrostatic interaction dominates the intrinsic bond strength of the M−M′ bonds. Furthermore, the increase of stability of the metal−metal bond with increasing atomic weight of the metal atoms M is due to an increase in the electrostatic contribution. The effective positive charge of the metal atoms are clearly enhanced by the more electronegative $NMe_2$ ligands, compared to the Cl ligands. Following the increase of the positive charge, the electrostatic contribution is getting larger, increasing by up to 65% for $(NMe_2)_3W-W(NMe_2)_3$. Although the orbital interaction contributes less to the total attractive interaction, one can identify two types of orbital interactions, one of $\sigma$- and one degenerate of $\pi$-symmetry. It is quite noticeable that the $\sigma$- and the two $\pi$-symmetric orbital interactions have almost the same strength in the $(NMe_2)_3M-M'(NMe_2)_3$ molecules, which means that the total $\pi$-bonding is much stronger than the $\sigma$-bonding. For the heteronuclear molecules, the bond strength as well as their components of the Pauli repulsion, and the electrostatic and orbital attraction always lies between the parent homonuclear molecules. The moderate charge transfer between the $MR_3$ and $M'R_3$ moieties does not alter the overall bonding picture significantly. CASPT2 calculations of **1Cl**−**3Cl** support the assignment of the molecules as triply bonded systems.

In conclusion, the M−M′ bonds in $R_3M-M'R_3$ may be classified as triple bonds with significantly stronger $\pi$-bonding than $\sigma$-bonding and a dominating quasiclassical contribution. The heterodimetallic species show only moderate polarity and their properties and stabilities are intermediate between the corresponding homodimetallic species, a fact that should allow for the experimental isolation of heterodinuclear species.

**Acknowledgment.** This work was supported by the Deutsche Forschungsgemeinschaft.

**Supporting Information Available:** This material is available free of charge via the Internet at http://pubs.acs.org.